First estimate of ambient hydroxyl radicals in the NW-IGP derived using in-situ measurements of aromatic VOCs and the toluene/benzene photo-chemical clock

Harshita Pawar

MS10075

A dissertation submitted for the partial fulfilment of
BS-MS dual degree in Science

Indian Institute of Science Education and Research Mohali
April 2015

Certificate of Examination

This is to certify that the dissertation entitled "**First estimate of ambient hydroxyl radicals in the NW-IGP derived using in-situ measurements of aromatic VOCs and the toluene/benzene photo-chemical clock**" submitted by **Ms. Harshita Pawar** (MS10075) for the partial fulfilment of BS-MS dual degree programme of the Institute, has been examined by the thesis committee duly appointed by the Institute. The committee finds the work done by the candidate satisfactory and recommends that the report be accepted.

Dr. V. Sinha (Supervisor)

Dr. B. Sinha

Dr. S. Ghosh

Dated: April 23, 2015

Declaration

The work presented in this dissertation has been carried out by me under the guidance of Dr. V. Sinha at the Indian Institute of Science Education and Research Mohali.

This work has not been submitted in part or in full for a degree, a diploma, or a fellowship to any other university or institute. Whenever contributions of others are involved, every effort is made to indicate this clearly, with due acknowledgement of collaborative research and discussions. This thesis is a bonafide record of original work done by me and all sources listed within have been detailed in the bibliography.

Harshita Pawar
(Candidate)

Dated: April 23, 2015

In my capacity as the supervisor of the candidate's project work, I certify that the above statements by the candidate are true to the best of my knowledge.

Dr. V. Sinha

(Supervisor)

Acknowledgment

I would like to express my gratitude to Dr. Vinayak Sinha, my project supervisor for his kind supervision and guidance in completing my dissertation. I would also like to thank Dr. N. Sathyamurthy, Director, IISER Mohali and Dr. Anand Bachawat, Dean R&D, IISER Mohali for providing a conducive environment which was very helpful for completing the thesis in time. I am thankful to Dr. Baerbel Sinha and Dr. Samrat Ghosh for providing their valuable inputs.

I also acknowledge my lab mates Chinmoy Sarkar, Vinod Kumar, Saryu Garg, B. Praphulla Chandra, Gaurav Sharma, Savita Dutta and Haseeb Hakkim for their assistance.

List of Figures

List of Tables

Notation (Abbreviations)

1.	VOC	Volatile Organic Compounds
2.	FAGE	Fluorescence Assay by Gas Expansion
3.	CIMS	Chemical Ionization Mass Spectrometry
4.	NW-IGP	North-west Indo-Gangetic Plain
5.	NMHC	Non-methane hydrocarbons

Content

Abstract

Aromatic volatile organic compounds, which are emitted primarily from anthropogenic sources are amongst the most reactive precursors of tropospheric ozone and secondary organic aerosol. Till date however, the ambient concentrations and diel variability of compounds such as benzene, toluene, xylenes and trimethylbenzenes remain poorly constrained over the Indian region. The concentration of ambient hydroxyl radicals that are the primary tropospheric oxidants and control the removal rates of climate and air quality relevant gases has also not been previously quantified at any Indian site.

Here, we address the aforementioned gaps in our understanding related to ambient aromatic compounds and hydroxyl radicals using a novel in-situ VOC and meteorological dataset measured at a sub-urban site in the NW-IGP during April-May 2012. The observed concentrations (average ± 1σ ambient variability) were as follows: benzene (1.6 ± 1.7 ppbV), toluene (2.7 ± 3.1 ppbV), xylenes (1.9 ± 2.3 ppbV) and trimethylbenzenes (1.1 ± 1.2 ppbV). These values were found to be comparable in magnitude to average summertime mixing ratios reported in Tokyo, (benzene: 1-4 ppbV, toluene: 3-9 ppbV, C8 aromatics: 1.3 ppbV, C9 aromatics: 0.3 ppbV) but in general higher than those reported in Houston, USA, (benzene: 0.6 ppbV, toluene: 0.8ppbv, xylene: 0.6 ppbV). The strongest sources of the aromatic VOCs at our site were found to be point sources (e.g. congested traffic intersections such as Tribune Chowk) located in the urban clusters of Chandigarh, Panchkula and Mohali. Analogous trends observed in the time series of benzene, toluene, C8 and C9 aromatics and a high-degree of inter-VOC correlation ($r^2 > 0.6$) showed that common sources drive their emission profiles. By applying a chemical kinetics "photochemical clock" method, that exploits the differential OH reactivity of toluene and benzene, their measured emission ratios at the urban fetch region and the measurement site, we derived an average ambient hydroxyl radical concentration of (17 ± 3) × 10^6 molecules cm^{-3} or 0.68 ± 0.001 pptV. This suggests that the ambient oxidising capacity is

similar to the oxidising capacity observed in sites at higher latitudes influenced by urban emissions such as New York where ambient hydroxyl radical concentrations of 20×10^6 molecules cm^{-3} were reported. As the ambient chemical mixture has high concentration of both reactive aromatic compounds and oxidants, the potential for chemical transformations and reactions of aromatic compounds to form aerosol and fuel ozone production locally on short time scales (few hours) appears to be particularly high and is important to consider for mitigation strategies.

Chapter 1

Introduction

1.1 Atmospheric aromatic VOCs: Sources, global budgets and health impacts

Organic compounds that have a vapor pressure greater than 0.01kPa at 298K and low boiling points (323K to 533K) at 1.013 bar pressure are collectively termed as Volatile Organic Compounds (VOCs). Globally, every year ~1300 TgC (Goldstein and Galbally, 2007) of chemically diverse VOCs are emitted into the atmosphere.

These emissions exert direct and indirect effects on the atmospheric reactivity, climate, human health and environment (Goldstein and Galbally, 2007). Out of these, aromatic species which amount to ~25 TgC/yr (Koppmann, 2008) by virtue of their anthropogenic sources are particularly dominant in the ambient air of urban and sub-urban cities. They constitute an important fraction (~20–30%, mass percent) of total non-methane hydrocarbons (NMHCs) in the urban atmosphere (Zhang et al., 2013). Among the aromatic VOCs, benzene, toluene, sum of C8 and sum of C9-aromatics form an important class. Figure 1.1.1 shows the chemical structure of benzene, toluene, isomeric C8 and C9-aromatics which are the aromatic VOCs that have been studied in this work.

The single largest source of benzene in the ambient atmosphere is the practice of biomass burning (~2.5TgC/yr) whereas for toluene and xylene, the single largest sources are industrial and fossil fuel usage (4.3TgC/yr and 3.5 TgC/yr respectively) as illustrated in Figure 1.1.2.

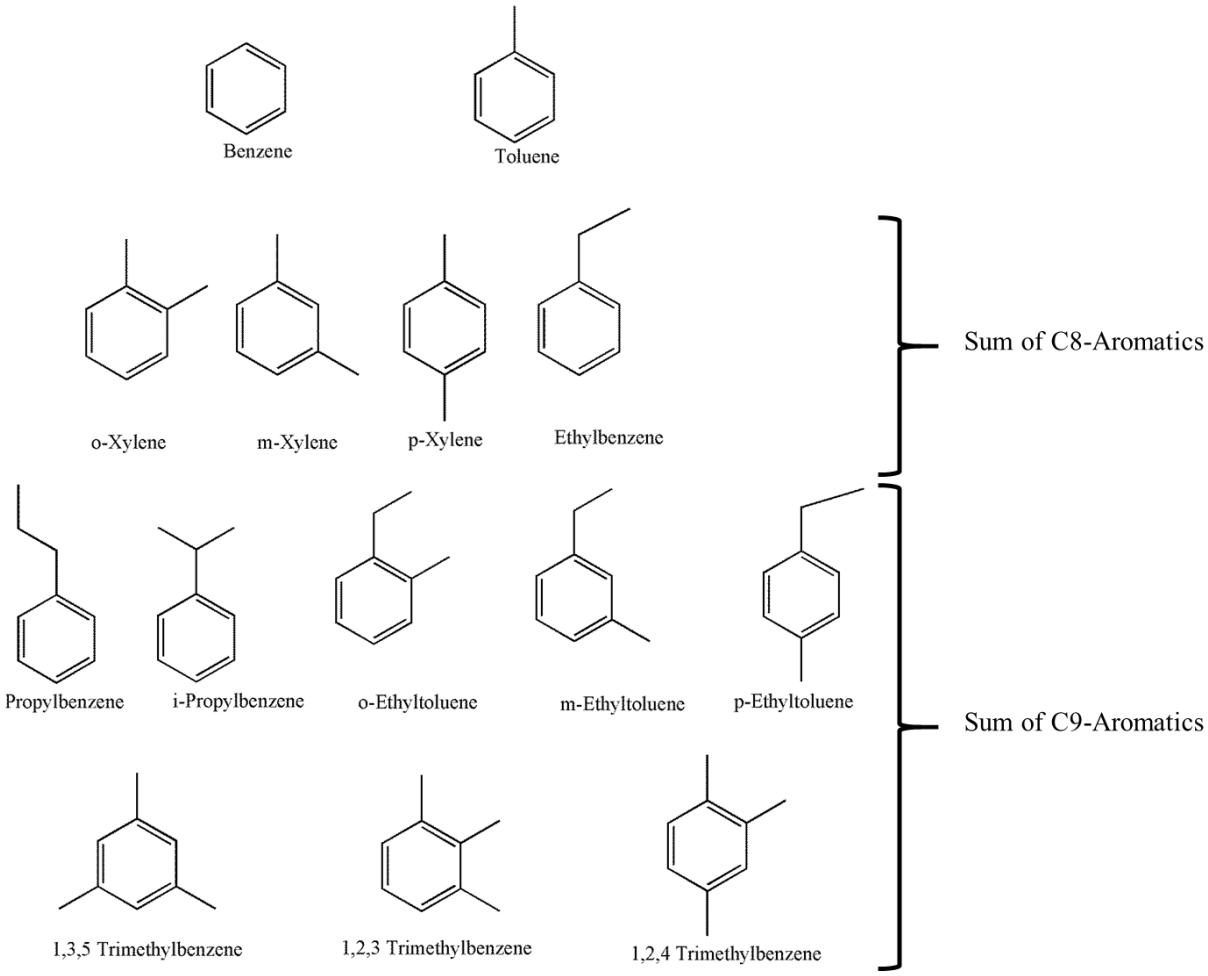

Figure 1.1.1: Chemical structure of benzene, toluene and isomers of C8 and C9 aromatics

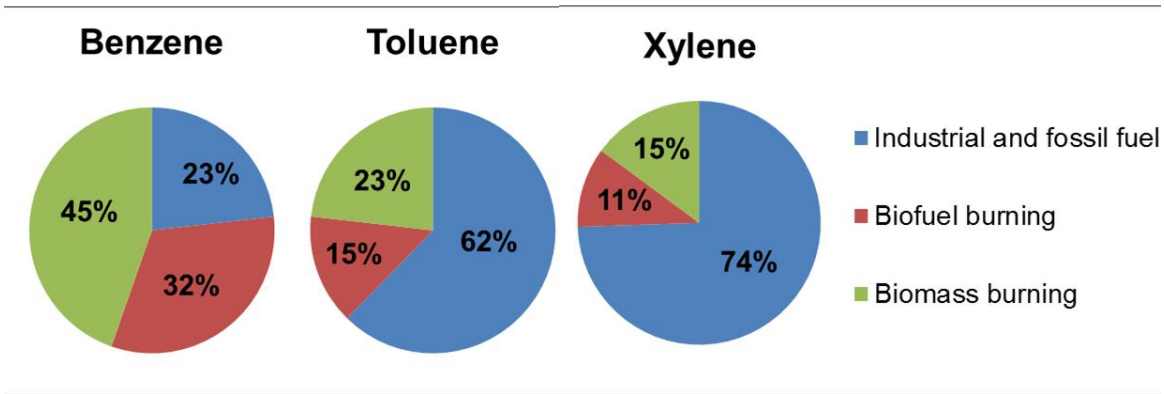

Figure 1.1.2: % emission of each aromatic specie broken down by source (Henze et al., 2008)

Aromatic hydrocarbons occur naturally in petro-chemicals. They are also used as solvents, gasoline additives and raw materials in the manufacturing consumer products such as paints, inks and plastics. Lignin, a complex polymer of aromatic alcohols is a primary constituent of wood and when wood is burnt as biomass, thermal degradation of lignin results in the emission of aromatic hydrocarbons into the atmosphere.

Aromatic VOCs are also associated with detrimental impact on human health. Benzene is a known human carcinogen for all routes of exposure. Chronic inhalation of benzene causes chromosomal aberrations and may lead to the development of aplastic anemia (WorldHealthOrganization, 2000). Chronic exposure of humans to toluene and xylenes causes irritation of the upper respiratory tract and eyes, sore throat, dizziness, and headache. Sustained exposure has also been known to cause central nervous system dysfunctions such as tremors and cardiac arrhythmia. Inhalation of the vapors of C9-aromatics is known to cause chemical pneumonitis, anxiety and asthamatic bronchitis. Exposure to aromatic VOCs also causes developmental defects such as limb anomalies. (Calabrese and Kenyon, 1991)

1.2 Role of aromatic VOCs in tropospheric chemistry

Once emitted into the atmosphere, reactivity of benzene, toluene, C8 and C9 aromatics with hydroxyl radical controls their removal rates. For aromatics with alkyl substituents (all except benzene), less than 10% of the reaction proceeds via H-abstraction from alkyl substituent which after a series of chemical reactions involving NOx and HOx yield a carbonyl compound.

The major reaction pathway of aromatic VOCs with hydroxyl radical proceeds mainly via the 1,2 addition of OH followed by O_2 to the aromatic ring to generate alkylperoxy adduct (RO_2).

This RO_2 radical follows three generic pathways to yield variety of products, the branching ratios of which are given in Table 1.1.1

i. ‘phenolic pathway’: RO_2 radical decomposes to form a hydroxyarene and HO_2
ii. ‘peroxide-bicyclic’ pathway: RO_2 radical isomerizes followed by ring closure to form a peroxide bridge which eventually yields a mixture of dicarbonyl products

iii. ‘epoxy-oxy’ route: Isomerization to form a cyclic epoxy-oxy radical that decomposes to give epoxydicarbonylene product

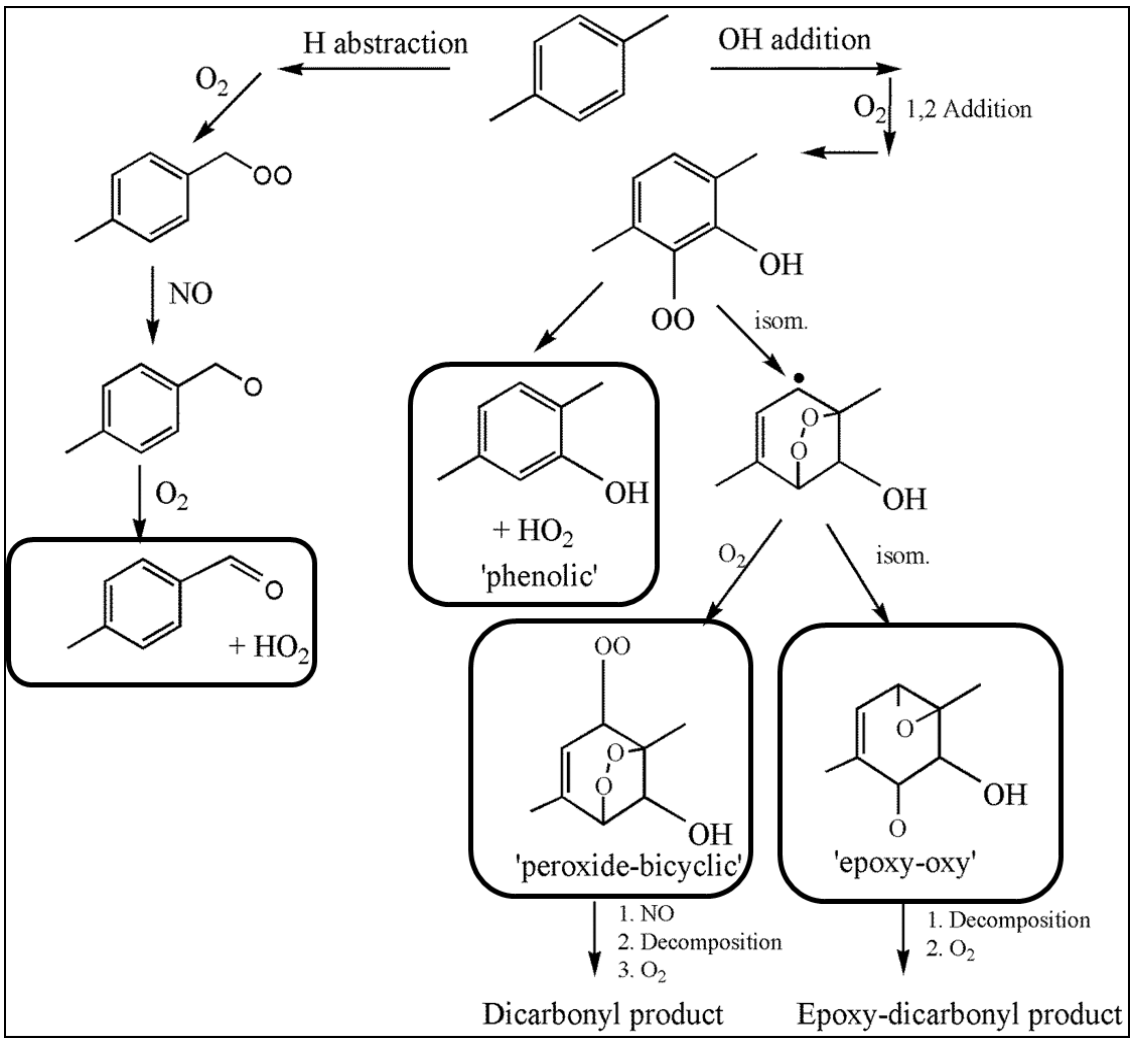

Figure 1.2.1: Degradation schematic of p-xylene with hydroxyl radical.(Bloss et al., 2005)

Table1.2.1 shows the relative branching ratios assigned to OH-initiated oxidation routes to first generation products. For all aromatic VOCs (except benzene), ‘peroxide-bicyclic’ is the major reaction pathway to yield dicarbonyl compounds as the major products.(Bloss et al., 2005;Jenkin et al., 2003). It should be noted that chemical reactions in the atmosphere converts hydrophobic aromatic VOC to hydrophilic phenolic of carbonyl moieties.

All reactions in which alkyl peroxy radical oxidizes NO to NO_2 are responsible for the formation of tropospheric ozone. The NO_2 photolyzes to give an O^3_P atom which combines with O_2 to give ozone.

Hydrocarbon	H abstraction	1,2 OH addition		
		phenolic	peroxide-bicyclic	epoxy-oxy
benzene	-	0.53	0.35	0.12
toluene	0.07	0.18	0.65	0.1
ethylbenzene	0.07	0.18	0.65	0.1
o-xylene	0.05	0.16	0.55	0.24
m-xylene	0.04	0.17	0.5	0.29
p-xylene	0.1	0.12	0.625	0.155
propylbenzene	0.07	0.18	0.65	0.1
i-propylbenzene	0.07	0.18	0.65	0.1
1,2,3-trimethylbenzene	0.06	0.03	0.7	0.21
1,2,4-trimethylbenzene	0.06	0.03	0.61	0.3
1,3,5-trimethylbenzene	0.03	0.04	0.79	0.14
o-ethyltoluene	0.05	0.16	0.55	0.24
m-ethyltoluene	0.04	0.17	0.5	0.29
p-ethyltoluene	0.1	0.12	0.625	0.155

Table1.2.1: Relative branching ratios assigned to OH-initiated oxidation routes to first generation products (Bloss et al., 2005)

Physical and chemical processing of aromatic VOCs converts them to less volatile products referred to as secondary organic aerosols (SOA) that condense in the particulate phase. Although estimated SOA from biogenic sources in natural environments is substantially higher than that from anthropogenic sources on the global scale, aromatic VOCs have been identified as dominant SOA precursors in populated urban and industrial places (Zhang et al., 2013). Because the oxidation products of aromatic VOCs are hydrophilic with high uptake of water, they are also responsible for the formation of photochemical smog.

Aromatic VOCs also lead to the formation of tropospheric ozone in photochemical reactions involving nitrogen oxides in the daytime. They have the higher photochemical ozone formation potential when compared with most alkanes and alkenes in urban environments. Aromatics alone were responsible for ~30% of tropospheric ozone in the boundary layer over Europe according to Derwent et al. (1998). High concentrations of ozone causes frequent exceedance from the air quality standards set for ozone (100 μgm^{-3}

for 8 hour average). It is also responsible for pulmonary disorders and enhanced crop yield loss.

1.3 Hydroxyl radical

Hydroxyl (OH) radicals control the self-cleansing capacity of the atmosphere. They determine the atmospheric lifetimes of major trace gases including those responsible for ozone depletion (HCFCs), greenhouse effect (CH_4). It prevents the accumulation of toxic species like CO and benzene in the atmosphere. Due to its importance, the concentration of OH radicals is also referred to as the oxidation capacity of the atmosphere. Short chemical lifetimes (~few milliseconds) because of high reactivity means that their budget is only controlled by local in-situ chemistry and not through transport. (Stone et al., 2012) The formation of hydroxyl radical initiates a series of gas phase radical-chain oxidation reactions.

Photolysis of ozone in the presence of water vapor is the main source of hydroxyl radicals in the troposphere

$$O_3 + h\upsilon\ (\lambda < 320nm) \longrightarrow O\ (^1D) + O_2\ (^1\Delta_g) \qquad (R1)$$

The fate of ~90% O (^1D) atoms is collisional quenching via

$$O\ (^1D) + N_2/O_2 \longrightarrow O\ (^3P) + N_2/O_2 \qquad (R2)$$

Up to 10% of O (^1D) reacts with water vapor to give two OH radicals

$$O\ (^1D) + H_2O \longrightarrow 2OH \qquad (R3)$$

Hydroxyl radical chemistry is coupled with hydroperoxy radical and collectively they are known as HO*x* (= OH + HO_2).

The major source of HO_2 is the reaction of hydroxyl radical with carbon monoxide.

$$OH + CO\ (+O_2) \longrightarrow HO_2 + CO_2 \qquad (R4)$$

Other dominant process that leads to the removal of tropospheric OH is through its reactions with methane and other VOCs (Monks, 2005, Lelieveld, 2004).

$$OH + RH + O_2 \longrightarrow RO_2 + H_2O_2 \qquad (R5)$$

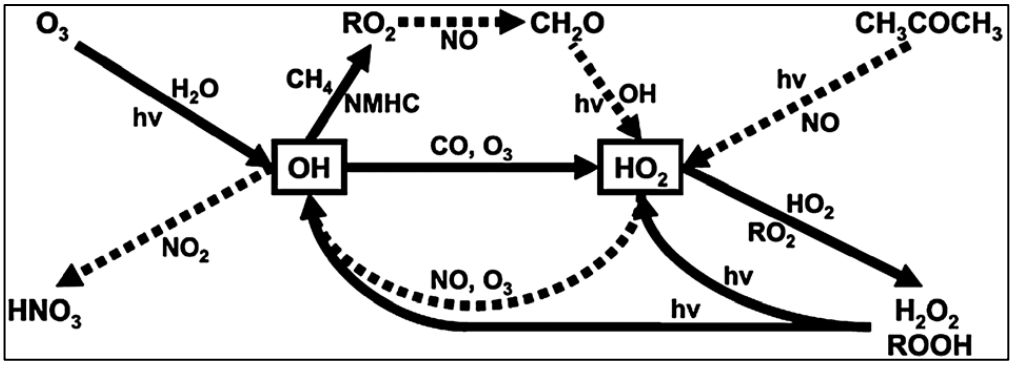

Figure1.3.1: The sources, sinks and inter-conversions of HO*x* and RO*x* in the troposphere (Stone et al., 2012). Pathways indicated by dashed lines are representative of high NOx (VOC limited regime): R10 and R11. Pathways indicated by solid lines represent process that dominate under background conditions.

In environments with low levels of NO (NO*x* limited), HO_2 reacts with ozone leading to the destruction of ozone and recycling of HO*x*.

$$HO_2 + O_3 \longrightarrow HO + 2O_2 \quad \text{(R6)}$$

$$OH + O_3 \longrightarrow HO_2 + O_2 \quad \text{(R7)}$$

The chain termination step is the reactions between peroxy radicals. (Lelieveld et al., 2004)

$$HO_2 + HO_2 \longrightarrow H_2O_2 + O_2 \quad \text{(R8)}$$

$$HO_2 + RO_2 \longrightarrow RO_2H + O_2 \quad \text{(R9)}$$

In environments with rich concentration of NO (VOC limited), the following reactions are compete over the reactions R8 and R9 and lead to the secondary production of OH radical

$$HO_2 + NO \longrightarrow HO + NO_2 \quad \text{(R10)}$$

$$RO_2 + NO \longrightarrow RO + NO_2 \quad \text{(R11)}$$

which eventually lead to the formation of tropospheric ozone via the reaction:

$$NO_2 + h\upsilon\ (\lambda < 420nm) \longrightarrow O\ (^3P) + NO \quad \text{(R12)}$$

$$O\ (^3P) + O_2 + M \longrightarrow O_3 + M \quad \text{(R13)}$$

First estimate of OH radical was given by Levy (1971) in 1971. In unpolluted pristine environments the main fate of hydroxyl radicals is reaction with either carbon monoxide or methane to produce peroxy radicals (R4 and R5). In more polluted environments dominated by NOx, reactions between HOx and NOx lead to the peroxy radical catalyzed

oxidation of NO to NO_2 which ultimately leads to the formation of tropospheric ozone (R10, R11, R12 and R13).

The major analytical techniques used for the measurement of tropospheric OH radicals are Fluorescence Assay by Gas Expansion (FAGE) and Chemical Ionization Mass Spectrometry (CIMS). FAGE uses a 266 nm laser source for inducing fluorescence at low pressure which is detected at 308 nm whereas in CIMS OH is first converted to isotopically labeled H_2SO_4 and then detected using mass spectrometry. (Stone et al., 2012)

In this study, we investigate the diel and spatial variability of aromatic volatile organic compounds in the NW IGP during April-May 2012 using a high temporal resolution dataset. After assessing the commonality of emission sources and photochemical processing which causes changes in the toluene/ benzene emission ratio, we apply relative rate kinetics for estimating the time-averaged hydroxyl radical concentration in Chandigarh city. The approach assumes that the species involved have a fixed background level, are emitted simultaneously from common sources and reaction with hydroxyl radical is the dominant degradation pathway. In this work by filtering the data for distinct traffic dominated source regions, we were able to satisfy these conditions and derive estimates for the ambient hydroxyl radical concentration. The results are then discussed in the context of chemical formation of surface ozone and secondary organic aerosol.

Chapter 2

Material and methods

2.1 Site description

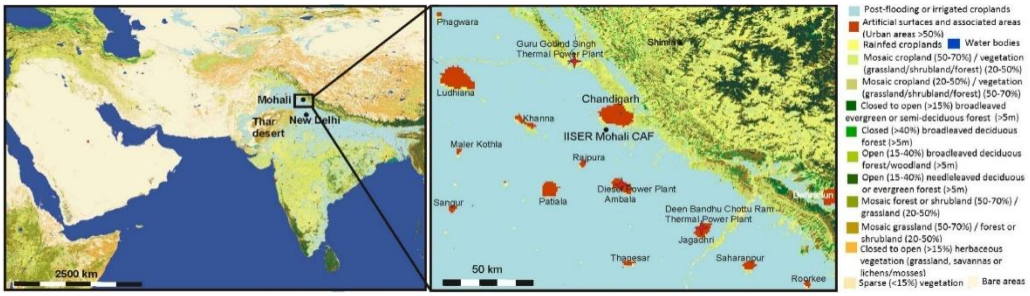

Figure 2.1.1: Left: Location of Mohali, in the NW-IGP. Right: Map of the land use in a 100 km×200 km area surrounding the measurement site (black dot, 30.667° N, 76.729°E, 310 m asl)

Figure 2.1.1(left) shows the location of the site in Mohali, super-imposed on a land-use map in the northwest Indo-Gangetic Plain close to the foothills of the Himalayan mountain range. The observations were carried out at the atmospheric chemistry facility of the Indian Institute of Science Education and Research (a sub-urban site in the city Mohali). Figure 2.1.1 (right) shows the precise location of the measurement facility and its spatial relationship with respect to neighboring cities and the Himalayan mountain range. The campus is mainly residential with tree cover and a few industrial units in the vicinity. The inlet used for PTR-MS was made of opaque Teflon tubing and was located at height of ~20m agl.

The wind sector spanning 0°-90° is primarily urban-industrial in land use. To the north-east of the measurement facility lies an urban-agglomeration of three cities: Chandigarh, Panchkula and Mohali collectively termed the tri-city. Figure 2.1.2 shows the spatial location of major traffic intersections and point sources of ambient aromatic VOCs in a

15 km × 15 km surrounding the measurement site. The major land use in other wind sectors is a mix of rural, agricultural and industrial.

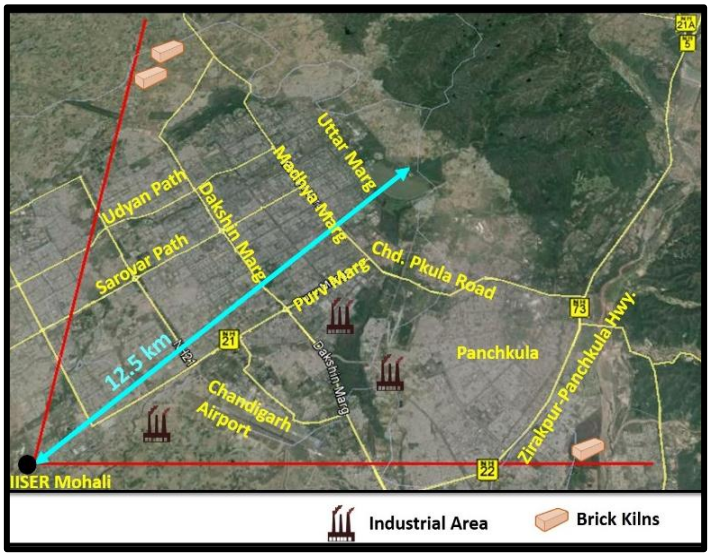

Figure 2.1.2: Google earth view of the major roads and point sources of ambient aromatic VOCs, 0° to 90°, in a 15 km × 15 km area surrounding the measurement site (black dot)

2.2 General meteorology

Wind speed, wind direction, ambient temperature and solar radiation were measured at the facility using meteorological sensors (Met One Instruments Inc., Rowlett, Texas, USA) at a temporal resolution of 1 minute. Figure 2.2.1 shows the wind rose plots for the period of study: April 1, 2012-May 31, 2012. Figure 2.2.2 shows the diel profile of the solar radiation, ambient temperature and relative humidity for the period of study along with their associated variability.

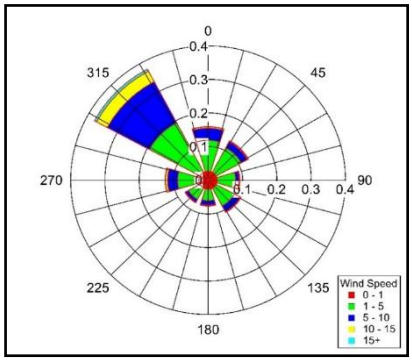

Figure 2.2.1: Wind rose plot for the measurement site (30.667N, 76.729 E, 310 ma.s.l.) for the period of April- May 2012.

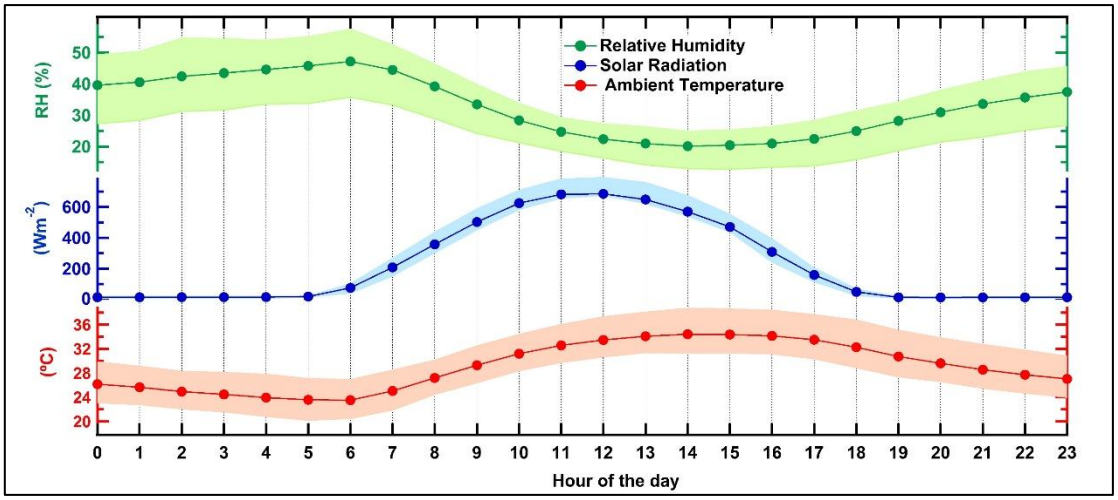

Figure 2.2.2: Diel profile of relative humidity, ambient temperature and solar radiation for the measurement site for the period of April- May 2012. Markers represent hourly average and the shaded region on the top and bottom represents the 75th and 25th percentile.

The months of April-May are associated with warm and dry days in which day-time average solar radiation peaked at ~600 Wm^{-2} between 11:00 and 14:00. The average ambient temperature also remained above 298 K except occasionally during early morning hours. The average daytime maximum temperature reached 34°C. The average maximum and minimum relative humidity varied between 47% at 06:00 till 20% at 14:00.

The duration of April-May were specifically chosen because cloudy days in monsoon (and eventually discontinuous solar radiation) and foggy days in winter, perturb the primary production pathway of hydroxyl radical and add to the complexity of analysis.

Conditions of calm (wind speed < 1 ms^{-1}) accounted for only 2.7% of the total duration and hence this period was suitable to analyze regionally representative concentrations of aromatic VOCs. Predominant wind direction during this time of the year is north to north westerly. This wind direction occurred ~54 % of the time during the period of study and coincided with the synoptic scale transport from the west. This fetch region was associated with high wind speeds and long range transport of particulate matter towards our site (Pawar et al., 2015).

Locally measured wind direction showed that the urban region (0°-90°) acted as fetch region of air masses only for ~20 % of the time. The advantage of real time measurements, was that we could select all data pertaining to this well-defined source sector and analyze it to derive an estimate of OH radical concentrations. Wind speeds for

this fetch region varied between 1 to 10 ms^{-1} for ~97% of the time. Higher wind speeds were observed occasionally during thunderstorms.

2.3 Volatile organic compound measurements using a proton transfer reaction mass spectrometer

High sensitivity proton-transfer reaction mass spectrometry (PTR-MS) was developed by Professor Werner Lindinger and co-workers at the University of Innsbruck in Austria in 1998(Lindinger et al., 1998). It works on the principle of soft chemical ionization and is able to quantify trace level volatile organic compounds present in the ambient air.

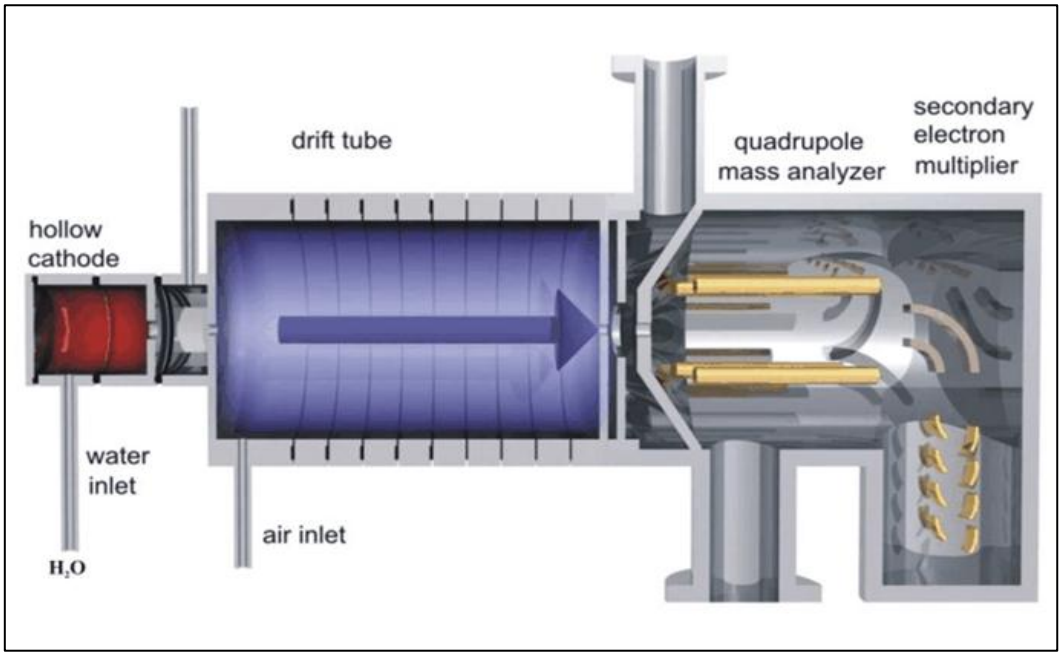

Figure 2.3.1 Schematic of the proton transfer reaction mass spectrometer

In this study, a high-sensitivity proton transfer reaction quadrupole mass spectrometer (HS Model 11-07HS-088; Ionicon Analytik Gesellschaft, Austria) was used for online measurements of selected volatile organic compounds. A detailed description of the instrument has been provided in Sinha et al. (2014). Here we present aspects relevant for the present dataset of measurements.

The four major parts of the PTR-MS shown in Figure 2.3.1 are:

1) Hollow cathode ion source: Production of highly pure H_3O^+ (>95%) reagent ions takes place by plasma discharge of water vapor by application of 450 V DC voltage

2) Drift-tube: Drift tube is made of stainless steel, separated by Teflon rings and resistors such that the potential across the entire drift tube length (~9.3 cm) is 600V. Inside the drift tube, soft chemical ionization of analyte molecules with proton affinity greater than that of water (e.g. VOCs) takes place as

$$H_3O^+ + RH \longrightarrow RH^+ + H_2O \qquad (R14)$$

where R is any analyte molecule and RH+ is the protonated molecular ion

3) Quadrupole mass analyzer that separates the protonated molecular ions according to their mass/charge (m/z) ratio

4) Secondary electron multiplier as a detector

The aromatic VOCs namely, benzene (C_6H_6; M.W. 78 g /mol), toluene (C_7H_8; M.W. 92 g /mol), C8- aromatics (C_8H_{10}; M.W. 106 g /mol) and C9- aromatics (C_9H_{12}; M.W. 120 g /mol) species were detected at their protonated ions: $C_6H_7^+$ (m/z=79), $C_7H_9^+$ (m/z=93), $C_8H_{11}^+$ (m/z=107) and $C_9H_{13}^+$ (m/z=121) respectively, after undergoing soft chemical ionization with hydronium ions.

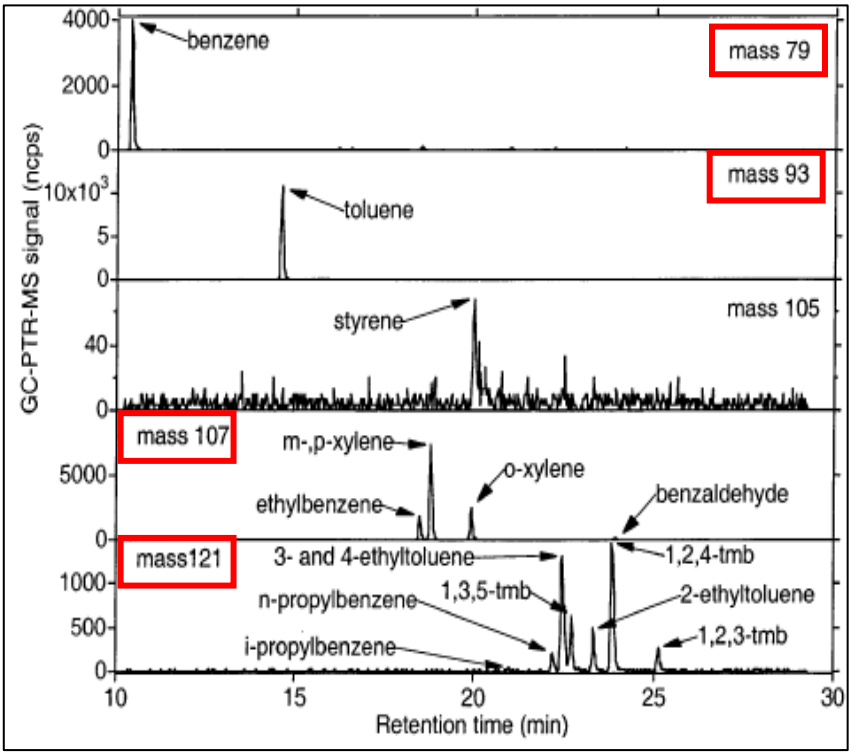

Figure 2.3.2: A typical GC-PTR-MS chromatogram for aromatic VOCs in ambient air (Warneke et al., 2003). The term 'tmb' stands for trimethylbenzene

It should be noted that the basis for compound attribution is mass of the measured protonated organic ion which in itself is not unambiguous. However, various validation studies ((Warneke et al., 2003), (De Gouw et al., 2003)) in a variety of environments where more specific techniques were coupled to or operated alongside the PTR-MS instrument have shown that these organic ions in ambient air have no other major contributor.

Figure 2.3.2 shows GC-PTR-MS chromatogram of aromatic VOCs for an ambient air sample. ((Warneke et al., 2003)). Here, a combination of gas chromatograph was (GC-PTR-MS) was used to validate the compound attribution. The air mixture was first separated using GC and detected using PTR-MS. At m/z 79 and m/z 93 benzene and toluene are the only contributor to the mass spectra. At m/z 107 and m/z 121 only isomeric C8 and C9 aromatics contribute to the mass spectra thus validating PTR-MS measurements.

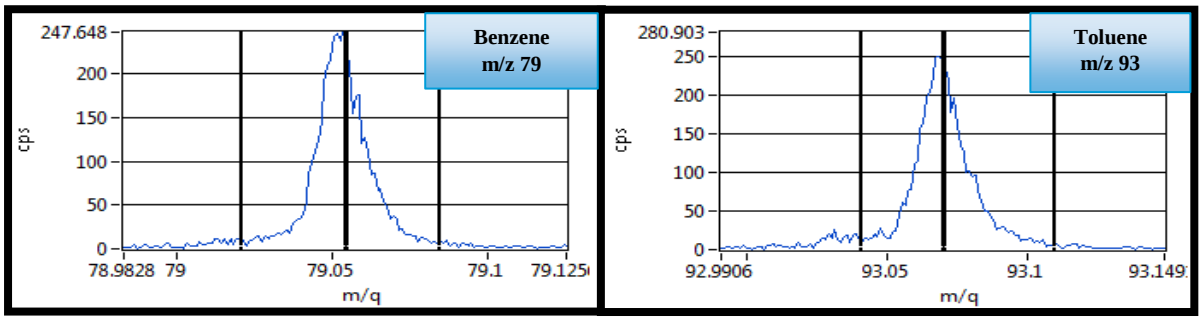

Figure 2.3.3: PTR-TOF-MS signal at m79 and m93 measured with PTR-TOF MS facility at Kathmandu. (Image courtesy: Chinmoy Sarkar, Atmospheric Chemistry and Emissions Group, IISER Mohali)

The compound attribution at m/z 79 and m/z 93 was also verified using a PTR-TOF-MS (time of flight mass spectrometer) facility at Kathmandu which provides an excellent mass resolution of up to 5000. Figure 2.3.3 shows the PTR-TOF-MS signal at m/z 79 and m/z 93 which again confirms the fact that benzene and toluene are the only contributors at that respective m/z channel.

2.4 Data quality assurance

2.4.1 Calibration procedure

To determine the sensitivity and limit of detection provided by PTR-MS for aromatic VOCs, calibrations were performed wherein high purity VOC calibration gas at different

flows was introduced after dynamically diluting it with a constant flow of VOC free zero air. Zero air was generated by passing synthetic zero air (Sigma gases; 99.9999% purity) over a Supelco activated charcoal tube and VOC scrubber catalyst (Gas calibration unit; Ionimed Analytik, Innsbruck, Austria, (Sinha et al., 2014)). PTR-MS signal observed while passing zero air was taken as the instrumental background. The slope of the plot between PTR-MS response in normalized counts per second (after correcting for zero background) and the introduced mixing ratio gave the sensitivity in ncps/ppbV.

Figure 2.4.1 shows the sensitivity (the parameter b in each image) and excellent linearity (r^2 = 0.99) for the PTR-MS calibration performed at 75% RH for all aromatic VOCs. The horizontal error bars represent the root mean square propagation of errors due to error in gas standards (6% each for benzene and toluene, 5% each for p-xylene and 1,2,4-trimethylbenzene) and 2% each error for the two mass flow controllers used during calibration. The vertical error bars represent 2σ instrumental precision error while sampling the standard gas at each dilution point. The total uncertainty was given as root mean square of accuracy error and precision error. Table 2.4.1 lists the VOC m/z assignments, sensitivity, detection limit and uncertainty for aromatic VOC used in this study the calibration plots for which are shown in Figure 2.4.1

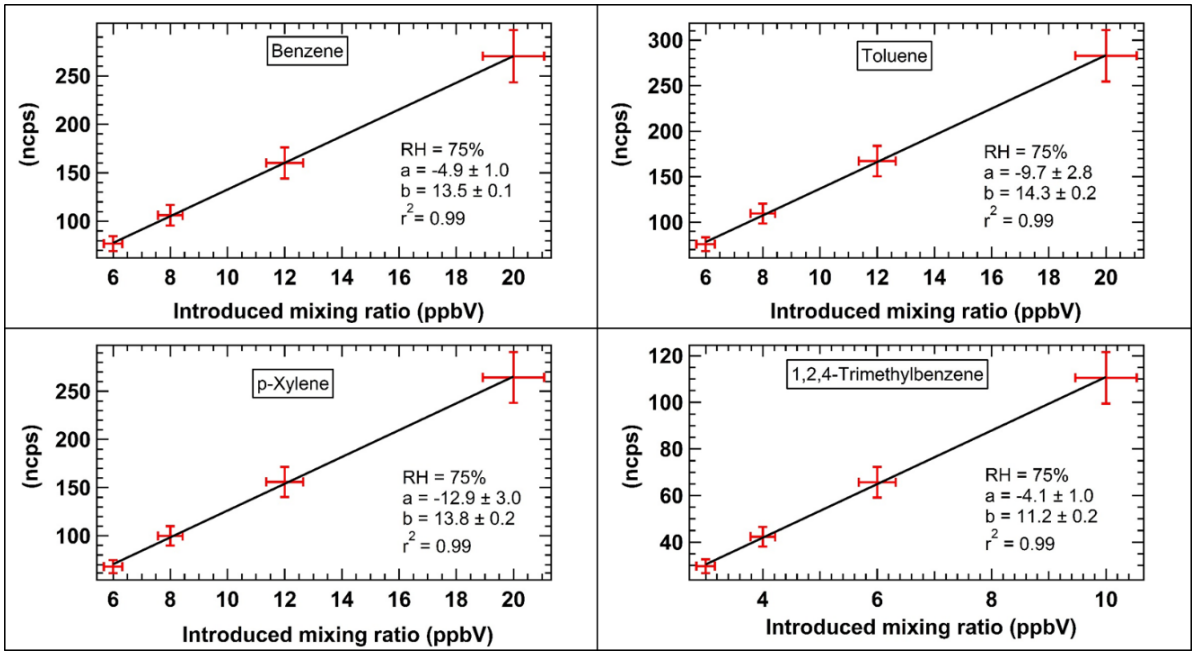

Figure 2.4.1: Sensitivity and linearity of aromatic VOCs in the PTR-MS calibration experiment performed. The y axis represents the response of PTR-MS in normalized counts per second (ncps) and the x axis is the introduced mixing ratio. The parameter 'b' in each of the above images is the sensitivity factor (ncps/ppb) for that particular VOC.

Hence, PTR-MS provides accurate measurements of aromatic VOC in the ambient air offering rapid response time and excellent detection limits. For this study, we used aromatic VOC measurements performed at a temporal resolution of 1 min during April-May 2012.

VOC	Nominal protonated (m/z)	Sensitivity (ncps/ppbV)	Limit of detection (ppbV)	Uncertainty
Benzene	79	13.5	0.07	9.5 %
Toluene	93	14.3	0.08	8.6 %
p-Xylene	107	13.8	0.10	10.8 %
1,2,4-Trimethyl benzene	121	11.2	0.13	11%

Table 2.4.1: Compound-specific aromatic VOC m/z assignments, sensitivity, detection limit and uncertainty.(Sinha et al., 2014)

2.4.2 Dataset optimization for aromatic VOCs

Local influences on the measurements from residences, hostel emissions and buildings in extreme vicinity are expected to be significant at low wind speeds (< $1ms^{-1}$, 2.7% of the dataset), and hence for the purpose of this study, aromatic VOC data pertaining to periods with wind speed ≥ 1 ms^{-1} (97.3 % of the dataset) was further analyzed.

2.4.3 Bivariate polar plots

Bivariate polar plots depict the variation in concentration of a specie with respect to wind speed and wind direction. The plots help give a graphical impression of potential sources that influences a location. To make the bivariate polar graphs, wind speed and wind direction data is segregated into bins of 1 ms^{-1} and 10° width respectively and the mean trace gas concentration for each bin is calculated. This results in a plot in Cartesian co-ordinates which is converted to polar co-ordinates and interpolated using the Kriging technique to furnish the desired bivariate plot.(Carslaw et al., 2006).

Some wind-speed and wind-direction bins have only few data points; particularly those at high wind speeds which can cause biases hence it is imperative to use a dataset that has statistically significant points in all bins.

Chapter 3

Results and discussion

3.1 Temporal trends of summertime aromatic VOCs

Figure 3.1.1 shows the time series of daily averaged ambient mixing ratios of benzene, toluene, C8-aromatics and C9 aromatics for April- May 2012. The shaded region in each plot corresponds to the 10th and 90th percentile respectively, indicating the daily ambient variability.

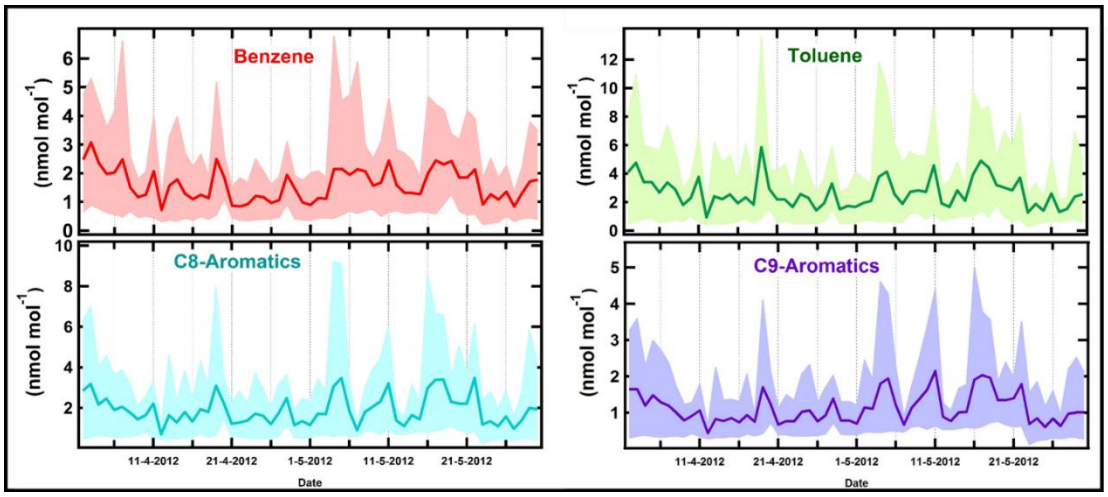

Figure 3.1.1: Time series of the daily averaged mixing ratios of benzene, toluene, C8-aromatics and C9-aromatics for April-May 2012. The top and bottom shaded region show 90th and 10th percentile respectively

For most of the duration of two months all aromatic VOCs exhibit analogous trends indicating that common sources drive their emission profiles. Table 3.1.1 shows the inter-VOC correlations calculated from the daily average values of benzene, toluene, C8-aromatics and C9-Aromatics (n = 61 in each case). The value of r^2 for each of the correlation between toluene, C-8 aromatics and C-9 aromatics is greater than 0.7 reflecting the co-emission of these compounds from similar sources (mainly traffic and industrial). Interestingly though benzene has a good correlation with each of these

compounds ($r^2 > 0.6$), due to the common urban sources, its correlation is lower due to the larger fraction of benzene released from biomass burning, a source that is not as dominant for the other aromatics(Henze et al., 2008).

	Benzene	Toluene	C8-Aromatics	C9-Aromatics
Benzene	1.00	-	-	-
Toluene	**0.7**	1.00	-	-
C8-Aromatics	**0.6**	**0.8**	1.00	-
C9-Aromatics	**0.6**	**0.8**	**0.9**	1.00

Table 3.1.1: Inter-aromatic VOC correlation for the average daily concentrations of benzene, toluene, sum of C8 aromatics and sum of C9 aromatics; r^2 values ≥ 0.5 are shown in bold.

The average ± 1σ ambient variability in mixing ratios of benzene (1.6 ± 1.7 ppbV), toluene (2.7 ± 3.1 ppbV), C8 (1.9 ± 2.3 ppbV) and C9 aromatics (1.1 ± 1.2 ppbV) for the period of study (April-May 2012) fall within the range of average summertime mixing ratios reported from other sites of the world. (Table 3.1.2)

	Mohali (2012)	Paris (2007) (Gros et al., 2011)	Mexico City (2003) (Lamb et al., 2004)	Tokyo (2002) (Kato et al., 2004)	Houston (2000) (Karl et al., 2003)
Benzene	1.6 (1.7)	1.2	1.7	1-4	0.6
Toluene	2.7 (3.1)	5.2	7.2	3-9	0.8
C8-Aromatics	1.9 (2.3)	5.5	3.3	1.3	0.6
C9-Aromatics	1.1 (1.2)	4		0.3	

Table 3.1.2: Average and standard deviation of aromatic VOCs measured at IISER Mohali in April-May 2012 and comparison with average levels reported in summertime from other cities of the world. The value in parenthesis indicates the standard deviation. All values are reported in nmol mol^{-1} (or ppbV).

The average daily concentrations during April- May 2012 ranged between 0.7 nmol mol^{-1} to 3.1 nmol mol^{-1} for benzene, 0.9 nmol mol^{-1} to 5.9 nmol mol^{-1} for toluene, 0.7 nmol mol^{-1} to 3.5 nmol mol^{-1} for C8-aromatics and 0.4 nmol mol^{-1} to 2.2 nmol mol^{-1} for C9-

aromatics. High variability in the levels of benzene, toluene, C8 and C9 aromatics were observed on May 7th, May 11th, May 16th and May 21st. These days corresponded to the time when plumes reached our site after passing over regions where wheat residue burning (Sinha et al., 2014) was active, a practice prevalent in most of the NW-IGP (Sarkar et al., 2013).

3.2 Diel concentration profiles of summertime aromatic VOCs

Figure 3.2.1 shows the diel plots of benzene, toluene, C8, and C9 aromatics. The solid line represents the hourly median concentration whereas the dotted lines represent the variability. In order to minimize the influence of very local events, time-periods with wind speed < 1ms^{-1} were filtered out.

	Lifetime due to		
	OH	**NO_3**	**O_3**
benzene	9.4 d	> 4 yr	> 4.5 yr
toluene	1.9 d	2.2 yr	> 4.5 yr
ethylbenzene	1.6 d	60 d	> 4.5 yr
m/p-xylene	7.4 h	105 d	> 4.5 yr
o-xylene	10.2 h	115 d	> 4.5 yr
i-propylbenzene	1.7 d	60 d	> 4.5 yr
propylbenzene	1.8 d	60 d	> 4.5 yr
m-ethyltoluene	7.2 h	60 d	> 4.5 yr
p-ethyltoluene	11.5 h	60 d	> 4.5 yr
1,2,4-trimethylbenzene	4.3 h	23 d	> 4.5 yr

Table 3.2.1: Lifetime of aromatic VOCs against oxidation with OH radical, NO_3 radical and O_3. Values are calculated based on rate constants from Atkinson and Arey (2003) and 12-hr daytime average OH radical concentration of 2 x 10^6 molecule cm^{-3}, for a 12-hr nighttime average NO_3 radical concentration of 5 x 10^8 molecules cm^{-3}, and for a 24-hr average O_3 concentration of 7 x 10^{11} molecules cm^{-3}.

All aromatic VOCs display a typical bimodal profile with a daytime minima and early morning and evening peak. During day-time, effective dilution due to elevated boundary

layer (~1500-2500m) results in low ambient concentrations. Moreover, photochemical oxidation of very reactive aromatic VOCs like xylenes (C8 aromatics), ethyltoluene and trimethylbenzene (C9-aromatics) (Table 3.2) with hydroxyl radical leads to further decrement in their ambient concentrations.

On the other hand at night, anthropogenic activities like biomass burning and evening traffic into a shallow nocturnal boundary (~50-100m) layer result in higher concentrations. It is worth mentioning that though both biomass burning and traffic contribute to aromatic VOCs, during the early morning hours 05:00 to 07:00 LT biomass burning due to open cooking fires appears to dominate over traffic sources. This can be seen in the diel profile of benzene and toluene (Figure 3.2.1), wherein the evening and morning peaks are of similar amplitude for benzene (due to strong emissions from both biomass burning and traffic sources) but the amplitude of the evening peak is much higher for toluene, xylenes and trimethylbenzenes (which are emitted more strongly by traffic sources relative to biomass burning sources).

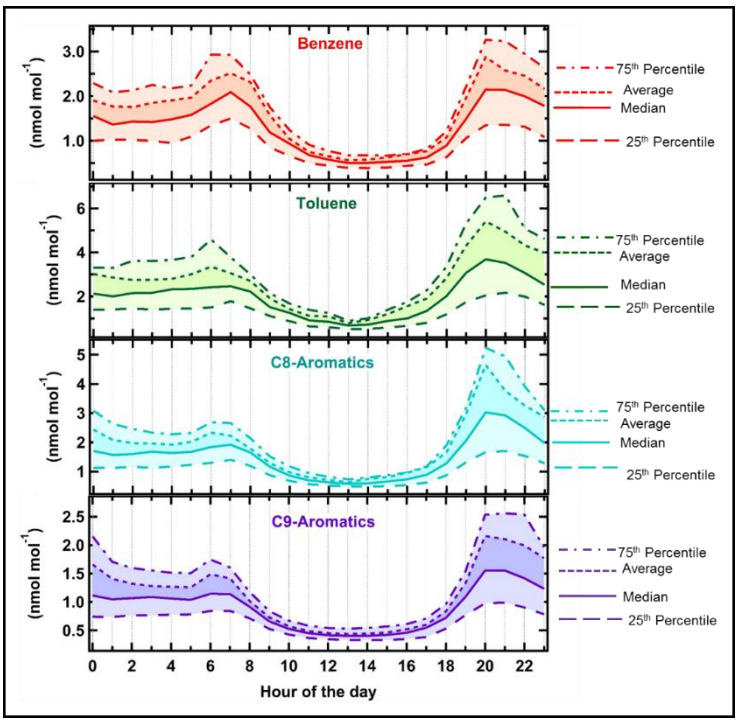

Figure 3.2.1: Diel profile of benzene, toluene, C8-aromatics and C9-Aromatics for April-May 2012.The solid line represents the hourly median value. The shaded region represents the variability.

3.3 Spatial analysis of summertime aromatic VOCs

Figure 3.3.1 shows the bivariate polar graphs for daytime and nighttime aromatic VOCs that helps elucidate the spatial hotspots of compound specific emission sources. Since wind direction at times with wind speed < 1ms^{-1} is not always meaningful and concentrations under such calm conditions are only representative of the extremely local sources (< 500 m), data corresponding to time periods with wind speed < 1ms^{-1} were excluded from the analysis. The study uses two months of data of aromatic VOCs measured at a high temporal resolution, some with high wind speeds (>15 ms^{-1}) as the meteorological conditions during storms are complex and squalls are poorly suited for identifying spatially fixed point sources. Only data points with wind speed between 1-15 ms^{-1} (~96% of the dataset) were considered for making these plots.

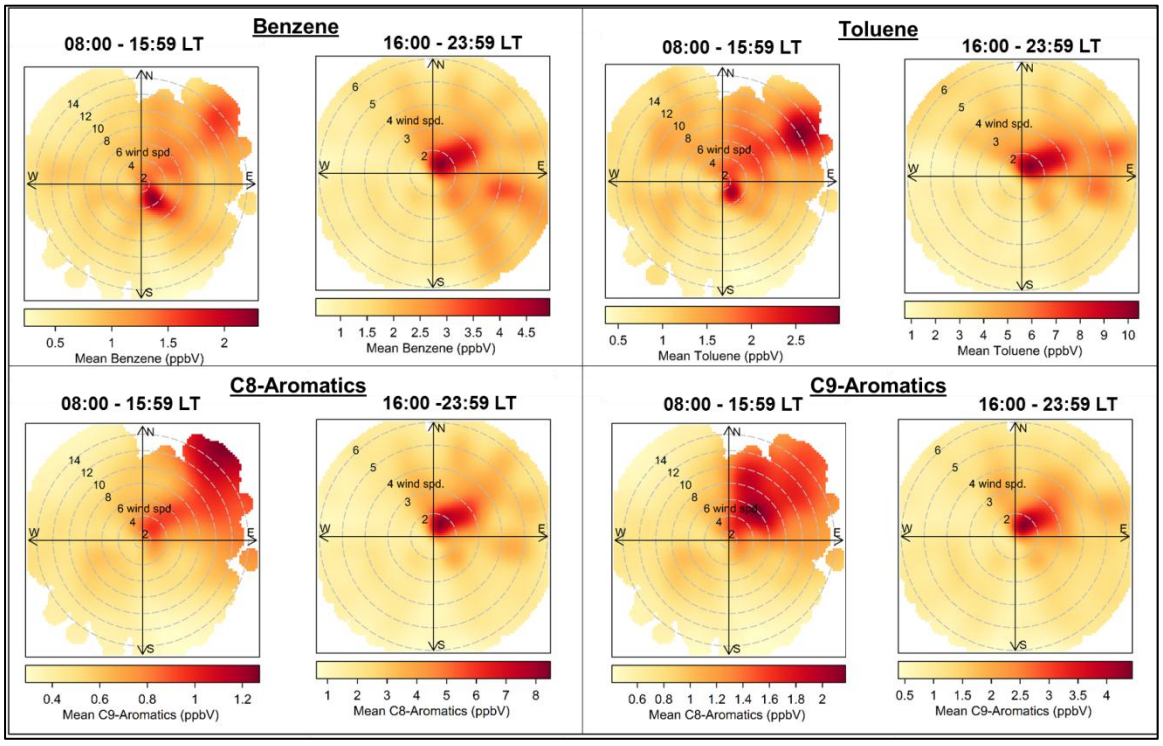

Figure 3.3.1: Day time (08:00 to 15:59 LT) and evening to night time (16:00 – 23:59 LT) bivariate polar plots of benzene, toluene, C8-aromatics and C9-Aromatics for April-May 2012

The daytime bivariate plots (Figure 3.1.3) point to emission hotspots in the north to north east fetch region for benzene, toluene, C8, and C9 aromatics, which is not entirely surprising considering that this wind sector represents the urban fetch region. The highest

mixing ratios of aromatic VOCs occurred predominantly in the north to north-east quadrant over all wind speeds $\geq 1ms^{-1}$ for all the compounds strongly suggesting the commonality of emission sources for the aromatic compounds.

While during daytime radiative heating from earth's surface promotes turbulence in the lower atmosphere resulting in higher wind speeds, periods between evening and night time (16:00 to 23:59) are associated with calmer conditions due to reduced turbulence. To illustrate the directional and spatial trend, only data periods with wind speeds $\geq 1ms^{-1}$ and $\leq 6ms^{-1}$ (~ 75% of data) were considered for the nighttime bivariate polar graphs. The evening to nighttime (16:00 to 23:59 LT) bivariate plots again elucidates the enhancement from urban region (north to north east quadrant). Although spatially the fetch region has reduced due to lower wind speeds, the directionality is preserved. The places in close vicinity to the measurement site are hot-spots of highest mixing ratios of all aromatic VOCs.

For all aromatic VOCs, average nighttime mixing ratios are notably higher than average daytime mixing ratios. This agrees well with the fact that higher wind speeds and elevated boundary layer height during the day time ensures greater dilution and hence lower mixing ratios. On the contrary, shallow boundary layer (~15 to 20 times smaller than day time boundary layer height) and lower wind speeds during nighttime result in higher mixing ratios.

3.4 Estimation of hydroxyl radical using toluene/benzene (T/B) photochemical clock

After emission into the atmosphere, volatile organic compounds are subjected to photochemical oxidation by hydroxyl radicals. Each reaction proceeds at a unique rate, depending on the OH reactivity of the aromatic compound. In a number of studies it has been shown that the change in emission ratios of compounds with different OH reactivities can be used to track the "photochemical age" of air masses (De Gouw et al., 2005;Parrish et al., 1992) or alternatively if the transport time is known can be used to estimate concentrations of hydroxyl radical concentration (Blake et al., 1993;Song et al., 2011).

As direct measurements of ambient hydroxyl radicals have never been performed before over any site in India due to the analytical challenges involved (e.g. low ambient hydroxyl

radical concentration at 0.1 pptV), due to the uniqueness of our measured dataset, we were able to estimate the average hydroxyl radical concentrations based on the change observed in toluene to benzene emission ratio.

We modified the approach by (Roberts et al. (1984)) Song et al. (2011), where they the ratio of aromatic VOCs with significantly different lifetimes such as ethylbenzene to m-xylene (Song et al. (2011)) and ethylbenzene to benzene or o-xylene to benzene ((Roberts et al., 1984)) to estimate the hydroxyl radical concentration. There are several pre-requisites that should be satisfied for this method to yield meaningful results. These are discussed below.

The species involved should have a fixed background level, be emitted simultaneously from similar sources and reaction with hydroxyl radical should be the dominant removal pathway. Using the ratio in comparison to the absolute values provides the advantage that ratio remains invariant to the effects of dilution during transport.

The similarity of sources of benzene and toluene in our dataset is affirmed by the correlation of daily average values of each of them (r^2 = *0.7*, Table 3.1.1). To further ensure a uniform fetch region we restricted this analysis only for the urban wind sector spanning 0° to 90° and wind speeds between 1-15 ms^{-1}, the hot spot of benzene and toluene sources both during day and. This increased the correlation coefficient between toluene and benzene to r^2 = 0.9 signifying the similarity of sources, most probably a mixture of traffic and urban emission activities.

The atmospheric lifetimes of both benzene and toluene are controlled by their reaction rate with hydroxyl radicals and other oxidants like ozone and nitrate radicals form only a minor sink (Atkinson and Arey, 2003). Table 3.4.1 shows the rate constant (at 298K) for the reaction of benzene and toluene with hydroxyl radicals, ozone and nitrate radicals. There are seven orders of magnitude difference between the rate constant of the gas phase reaction of benzene and toluene with hydroxyl radical respectively and the other atmospheric oxidants.

Toluene, because of the presence of alkyl group is more reactive than benzene to reaction with the hydroxyl radical. Figure 2.2.2 shows the diel profile of average ambient temperature which always remained above 298 K (25° C) except for early morning hours (02:00 to 07:00 UTC) and varied between 23.52 ° C to 34.42 ° C. The rate constant of

reaction of benzene and toluene with hydroxyl radical was corrected of the temperature variation at our site using the Arrhenius equation:

$$k = Ae^{-B/T}$$

where *k* is the rate constant, A and B are the temperature dependent kinetic factors. The values of these parameters are mentioned in Table 3.4.1.

		OH Radical		
	$k_{OH+B/T}$	A	B	lifetime
benzene	1.22×10^{12}	2.33×10^{12}	193	9.4 days
toluene	5.63×10^{12}	1.81×10^{12}	-338	1.9 days
		O_3		
	$k_{O_3+B/T}$	A	B	lifetime
benzene	$< 1.0 \times 10^{-20}$	-	-	> 4.5 yr
toluene	$< 1.0 \times 10^{-20}$	-	-	> 4.5 yr
		NO_3 Radical		
	$k_{NO_3+B/T}$	A	B	lifetime
benzene	$< 3 \times 10^{-17}$	-	-	> 4 yr
toluene	$< 3 \times 10^{-17}$	-	-	> 2.2 yr

Table 3.4: Room-temperature rate constants (*k* in $cm^3 molecule^{-1} s^{-1}$) and temperature dependent kinetic parameters, A ($cm^3 molecule^{-1} s^{-1}$) and B (K) of the gas-phase reaction of benzene and toluene with OH radical, O_3 and NO_3 radical. Values in the table are adapted from Atkinson and Arey (2003) Atkinson and Arey (2003) and references therein. '-' indicates that the parameters for the respective reactions have not been measured.

The mean OH radical concentration could be estimated from the method as:

$$ln\left(\frac{C_T'}{C_B'}\right) - ln\left(\frac{C_T}{C_B}\right) = (k_B - k_T) \times [OH] \times (t_2 - t_1)$$

where $\left(\frac{C_T'}{C_B'}\right)$ and $\left(\frac{C_T}{C_B}\right)$ are the measured ratios of toluene to benzene at the measurement site and at the source respectively, k_b and k_t are the temperature-corrected rate constants of the reaction of benzene and toluene with hydroxyl radical respectively and $(t_2 - t_1)$ is the transport time required by the air parcel to traverse from the source to the receptor site. $(t_2 - t_1)$. Based on the distance of the site from the agglomerate of urban sources in Figure 2.1.1, the distance was assumed to be 12.5 km. Dividing the distance by the average wind speed during that period pertaining to these data points yielded a transport time in seconds. It should be noted that the transport time represents the largest inherent uncertainty in this method.

3.4.1 Application of the T/B kinetics method to individual plumes arriving at the site

The wind-rose plot for the measurement site suggested that air mass transport from the urban fetch region occurred for ~20% of the time. So out of that duration, four specific events each during the daytime (08:00 to 15:59) and evening to night-time (16:00 to 23:59) were chosen from the period of April-May 2012 where our site received sustained plumes from the urban fetch region (0°–90°) with wind speeds between 1-15ms^{-1} advecting emissions from the urban fetch region. By choosing these events, we have to a very large extent ensured a first-hand check on the spatial commonality of sources and hence fulfilled the pre-requisite.

Figure 3.4.1a and b shows the excellent correlation between toluene and benzene for all eight events ($r^2 > 0.6$) which authenticated the commonality of sources for both benzene and toluene. Table 3.4.1a illustrates the day time events, the duration for which they lasted, the toluene to benzene emission ratio, the average wind speed, average ambient temperature and the temperature corrected rate constants of the reaction of toluene and benzene with hydroxyl radical. Table 3.4.1b lists the duration and toluene to benzene emission ratio for evening to night time events. The most important sink of toluene and benzene, i.e. the hydroxyl radicals are only photo-chemically produced during daytime. Hence, in the nighttime, because of the absence of an active sink, air parcels reaching our site from the urban fetch region will preserve the source signature along with the associated emission ratio. As expected, because of different reactivities of toluene and

benzene towards hydroxyl radical lower toluene to benzene emission ratio were observed for daytime (varying from 1.46 to 1.66) than evening to night time events (varying from 1.79 to 1.93).

It should be noted that, the nighttime toluene to benzene ratio currently used as a proxy for the source (Table 3.4.1c) are consistent with emission ratios reported in urban sites such as Beijing (varying from 1.5 to 2.2) (Liu et al. (2009) and Delhi (varying from 1.8 to 2.5) (Hoque et al. (2008)). T/B ratios reported from urban sites in developed countries are much higher (greater than 3) possibly because of more stringent controls on vehicle fleet and fuel grade, due to stricter regulation of benzene content in the fuels. We note that for India urban sites, reality would be closer to that of urban sites in similarly developing countries.

Date	Time	Toluene / Benzene	WS (ms^{-1})	T (°C)	k_{OH+B} (cm^3 molecule $^{-1}$ s^{-1})	k_{OH+T} (cm^3 molecule $^{-1}$ s^{-1})
April 01, 12	08:00-08:40	1.66	2.61	24.64	1.219×10^{-12}	5.631×10^{-12}
April 16, 12	10:21-15:59	1.46	6.58	26.60	1.224×10^{-12}	5.590×10^{-12}
April 26, 12	14:00-15:39	1.57	6.19	27.13	1.225×10^{-12}	5.579×10^{-12}
May 20, 12	09:50-12:14	1.58	6.34	35.11	1.246×10^{-12}	5.418×10^{-12}

Table 3.4.1a: Toluene to benzene emission ratio, average wind speed (WS), ambient temperature (T) and the temperature corrected rate-constant of the reaction of toluene or benzene with hydroxyl radical for the selected daytime events when measurement site received urban plumes (0° to 90°)

Date	Time	Toluene / Benzene
April 01, 12	20:20-23:53	1.93
May 01, 12	20:00-23:59	1.80
May 04, 12	18:47-23:08	1.86
May 17, 12	16:38-17:32	1.79

Table 3.4.1b: Toluene to benzene emission ratio for the selected nighttime events when measurement site received urban plumes (0°-90°)

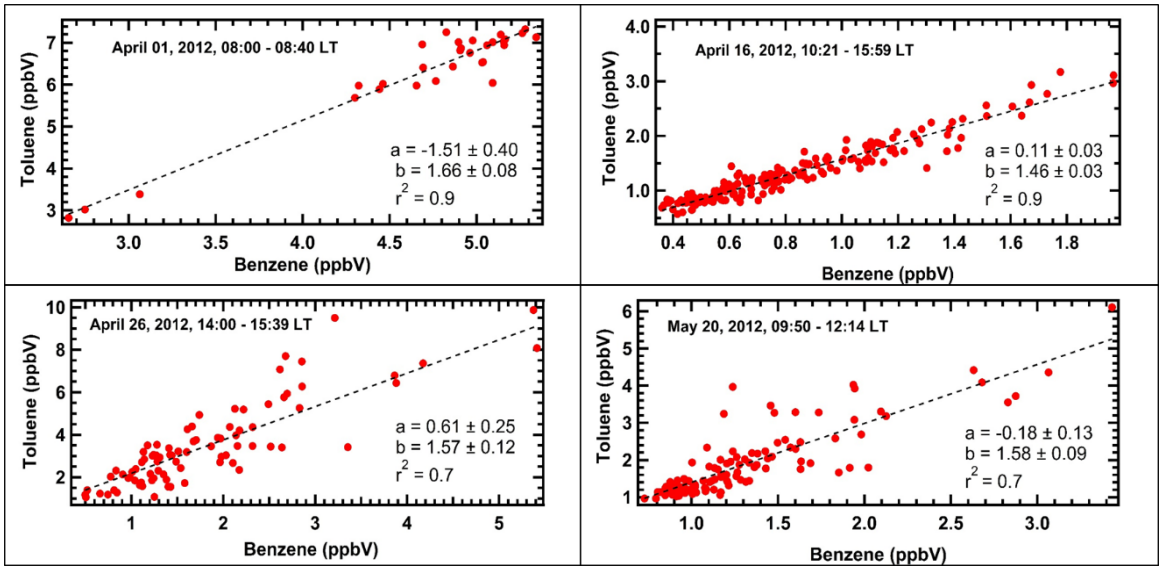

Figure 3.4.1a: Correlation plots of toluene and benzene for daytime events when measurement site received urban plumes (0° to 90°) and the wind speed was between 1-15 ms^{-1}. The toluene to benzene emission ratio is given by the parameter 'b' in the above image.

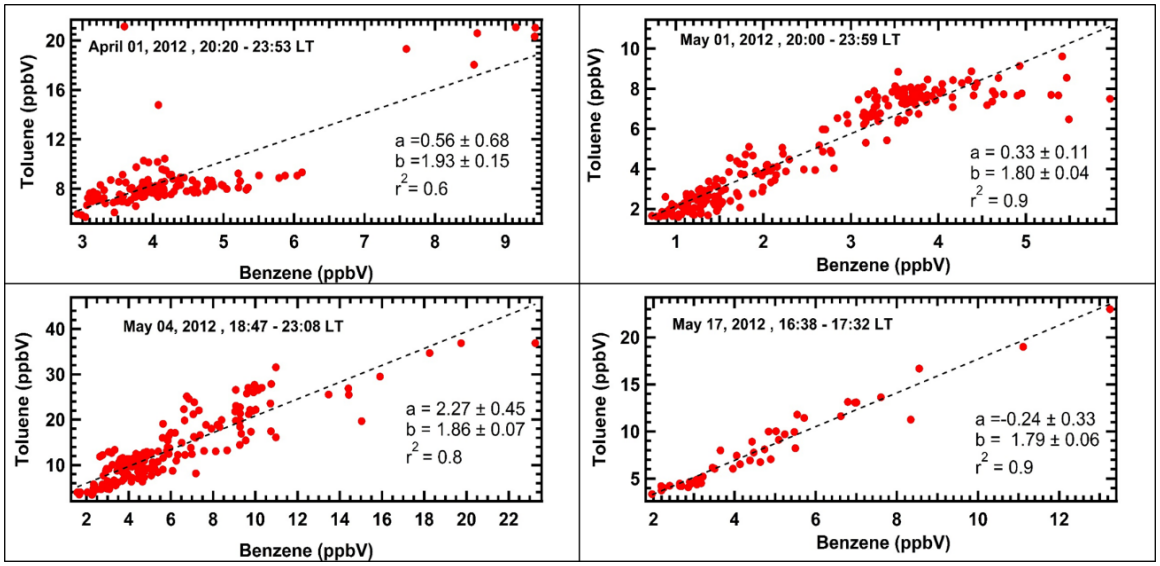

Figure 3.4.1b: Correlation plots of toluene and benzene for nighttime events when measurement site received urban plumes (0° to 90°) and the wind speed was between 1-15 ms^{-1}. The toluene to benzene ratio is given by the parameter 'b' in the above image.

Using the method described in section above we compute the time averaged hydroxyl radical number density using all possible combinations of the daytime versus night-time toluene to benzene ratios. The values ranged from 3.6×10^6 molecules cm^{-3} to 31.7×10^6 molecules cm^{-3} whereas the average was $(17.4 \pm 3.5) \times 10^6$ molecules cm^{-3}

Measurement Site	Toluene / Benzene
Mohali (India	1.6-2.3
Delhi (India) (Hoque et al., 2008)	1.8-2.5
Beijing (China) (Liu et al., 2009)	1.5-2.2
Belgium (Buczynska et al., 2009)	3.8-4.4
Canosa di Puglia (Italy) (Bruno et al., 2008)	3.4
Winsdor (Canada) (Miller et al., 2012)	4.3
Great Cairo (Khoder, 2007)	1.29 (rural)
	2.45 (urban)

Table 3.4.1c: Toluene/benzene levels as reported in previous studies

3.4.2 Estimation of hydroxyl radical using the average diel profiles of toluene to benzene ratio

For most of the hours of the day except the evening there was a close agreement between the average and the median ratios which throws light on the fact that by choosing only the urban fetch region we carefully limited the sources of ambient toluene and benzene.

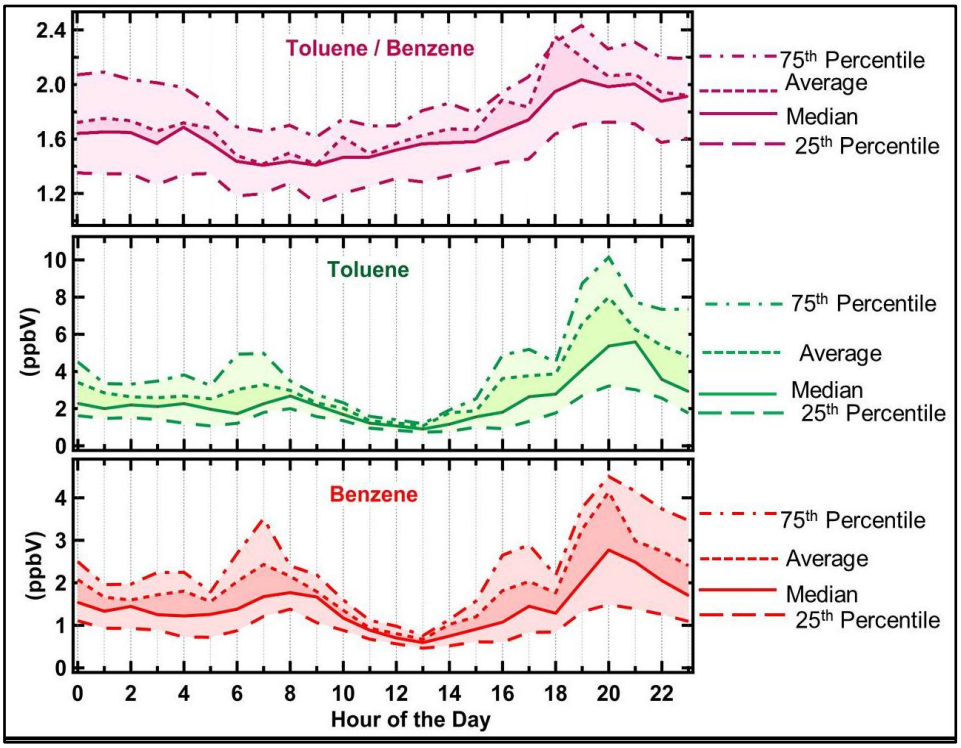

Figure 3.4.2: Diel profile of toluene to benzene ratio, toluene and benzene filtered for the urban fetch region and wind speed 1-15 ms^{-1}

Both toluene and benzene depict a typical bimodal profile (Figure 3.4.2) with peaks in early morning and evening and a daytime minima. Toluene being more reactive with hydroxyl radical would be oxidized more efficiently during daytime as compared to benzene and hence we expect to see a lower toluene to benzene ratio during the daytime. Figure 3.4.2 corroborates the same. Lower median toluene to benzene ratios, varying from 1.41 to 1.58 were observed during the daytime (08:00 to 15:59 LT) which could be attributed to a higher concentration of hydroxyl radicals. On the other hand, the median toluene to benzene ratios started increasing from 1600 LT due to increasing traffic density and decreasing hydroxyl radical sink. (varying from 1.66 to 2.03)

We used Levene's test for homogeneity of variance based on means and the pair wise comparison based on Tukey's studentised HSD test (Honestly Significant Differences) for assessing the statistical significance of the difference of the mean for each pair of hour of the day. The results suggest that the day time toluene to benzene ratios for each pair of hour between 08:00 and 15:59 were significantly lower than the evening to night-time ratios for each pair of hour between 16:00 and 23:59.

The ambient VOCs in the air masses reaching our site from the urban wind sector during evening to night time would preserve the signature of the source because of the absence of the major sink, the hydroxyl radical which is photo-chemically produced. Therefore, these toluene to benzene ratios would serve as a good proxy for the source ratio.

The ambient VOCs in the air masses reaching the receptor site from the urban wind sector during the daytime would be susceptible to reaction with the ambient hydroxyl radical. Therefore for $\left(\frac{C_T}{C_B}\right)$ we put to use the evening to night time ratios (16:00-23:59 LT) of toluene to benzene and for $\left(\frac{C_T'}{C_B'}\right)$ we use the day time ratio (08:00-15:59 LT).

Using this information and every possible combination of the ratios of toluene to benzene time averaged hydroxyl radical concentration was estimated. The values of time averaged hydroxyl radical number density ranged from 4.0×10^6 molecules cm^{-3} to 30.6×10^6 molecules cm^{-3} whereas the average was $(17.5 \pm 3.2) \times 10^6$ molecules cm^{-3}.

Hour of the day	Toluene / Benzene	WS (ms^{-1})	T (°C)	k_{OH+B} (cm^3 molecule $^{-1}$ s^{-1})	k_{OH+T} (cm^3 molecule $^{-1}$ s^{-1})
08:00-08:59 LT	1.42	2.99	27.20	1.225×10^{-12}	5.577×10^{-12}
09:00-09:59 LT	1.41	4.45	29.30	1.231×10^{-12}	5.534×10^{-12}
10:00-10:59 LT	1.46	4.19	31.21	1.236×10^{-12}	5.495×10^{-12}
11:00-11:59 LT	1.47	4.85	32.58	1.239×10^{-12}	5.468×10^{-12}
12:00-12:59 LT	1.52	3.48	33.49	1.242×10^{-12}	5.450×10^{-12}
13:00-13:59 LT	1.56	3.66	34.10	1.243×10^{-12}	5.438×10^{-12}
14:00-14:59 LT	1.57	4.26	34.42	1.244×10^{-12}	5.432×10^{-12}
15:00-15:59 LT	1.58	5.42	34.38	1.24×10^{-12}	5.433×10^{-12}

Table 3.4.2a: The median daytime (08:00 to 15:59) values of toluene to benzene (C_t/C_b) ratio, the average hourly wind speed, average hourly temperature and the temperature corrected rate constant of the reaction between toluene to benzene with hydroxyl radical.

Hour of the day	Toluene / Benzene
16:00-16:59 LT	1.66
17:00-17:59 LT	1.74
18:00-18:59 LT	1.95
19:00-19:59 LT	2.03
20:00-20:59 LT	1.98
21:00-21:59 LT	2.00
22:00-22:59 LT	1.88
23:00-23:59 LT	1.91

Table 3.4.2b: The median nighttime (16:00 to 23:59) values of toluene to benzene ratio

3.5 Comparison of estimated hydroxyl radical with other reported measurements

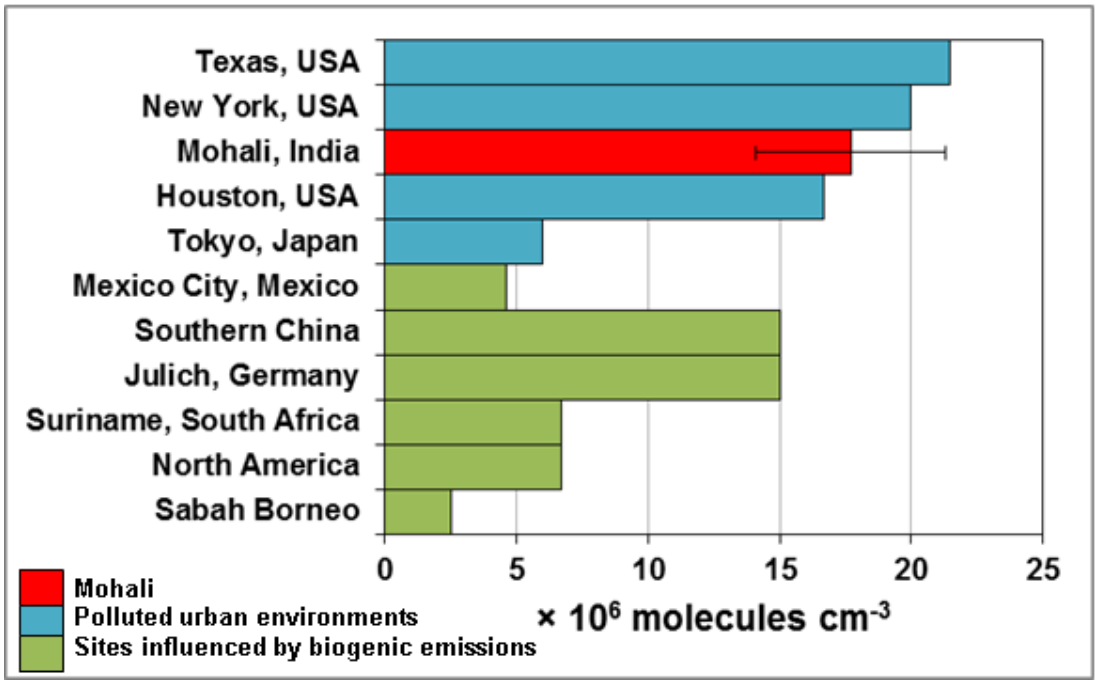

Figure 3.5: Comparison of hydroxyl radical concentration estimated for Mohali with values reported for other sites around the world(Stone et al., 2012)

The hydroxyl radical concentration estimated for Mohali compares well with urban sites in the world where HOx chemistry is dominated by NOx. Currently, models make use of

the global average hydroxyl radical concentration (~10^6 molecules cm^{-3}) to estimate the lifetime of trace gases. The estimated OH concentration, reduces the chemical lifetime of methane to 6 ± 3 months as compared to the global average of 8.7 years and for carbon monoxide to about 3.5 ± 2.1 days as opposed to global average lifetime of 60 days (2 months).(Warneck and Williams, 2012) This is close to the lifetimes obtained for urban sites elsewhere in the world (e.g. New York). Note however the reduction in the chemical lifetimes of long lived gases like methane and carbon monoxide does not occur to significant extent globally as transport and mixing processes do not permit the gases to remain over urban sites and instead they are distributed by advection and convection to regions that have only background hydroxyl radicals concentrations (~10^6 molecules cm^{-3}). Still, the fact that atmospheric chemistry over urban sites changes to cope with enhanced anthropogenic emissions of reactive compounds does capture the tendency for enhanced atmospheric self-cleansing capacity over the urban regions, which are rich in NO_x.

Chapter 4

Summary and conclusion

A novel in-situ data set on aromatic VOCs, benzene, toluene, C8 aromatics and C9 aromatics has been acquired for the months of April-May 2012 at a temporal resolution of 1 minute using a high sensitivity proton transfer reaction mass spectrometer. Using these measurements spatial and temporal variations of aromatic VOCs were investigated. Levels of aromatic VOCs observed for Mohali fall within the range of those reported from other sites in the world in similar seasons. Analogous trends in the time series of benzene, toluene, C8 and C9 aromatics and a high-degree of inter-VOC correlation illustrate that common sources drive their emission profiles. By combining measurements of VOCs and meteorological parameters at a representative site in the North West Indo-Gangetic plain we were able to identify that the strong point sources of aromatic VOCs were from the urban sectors of Chandigarh, Panchkula and Mohali. The observed toluene to benzene emission ratio (1.6-2.0) was close to values observed at sites in other developing countries like China (1.5-2.2) and Egypt (1.3-2.5).

After assessing the feasibility of applying a photochemical clock in the form of toluene/benzene emission ratios, which makes use of the difference in the reactivities of toluene and benzene towards oxidation with hydroxyl radical, a first estimate of the hydroxyl radical concentration was obtained for an Indian site influenced by urban emissions. This study reports a time-averaged OH radical concentration of $(17 \pm 3) \times 10^6$ molecules cm^{-3} which suggests similar oxidising capacity of local atmosphere to other sites influenced by urban emissions such as New York. Estimated OH radical concentrations are about ~17 times higher than the global average of 10^6 molecules $cm^{-3.}$ This could be explained because of strong solar radiation (maximum ~600 Watts m^{-2}) and secondary production of hydroxyl radicals in NO_x rich air during the summer months of April and May. One of the largest potential sources of uncertainty in the present study is

the calculated transport time of air masses from the urban source region to the measurement site. In future studies, use of a second pair of co-emitted hydrocarbons with differing OH reactivities (e.g. n-butane and iso-butane) could help overcome the large uncertainty and constrain the ambient hydroxyl radical concentrations better.

Estimated OH radical concentrations have been used to show that the chemical lifetime of methane (a greenhouse gas) and carbon monoxide (air pollutant) over urban sites is significantly lower than their global average lifetimes. Similar studies at suitable sites elsewhere in India would help determine the lifetime of greenhouse gases and air pollutants more accurately over the Indian region.

This study has contributed with novel results for the first time in India pertaining to basic OH radical chemistry through a comprehensive set of measurements of aromatic VOCs at a regionally representative site. As the ambient chemical mixture has high concentrations of both reactive aromatic compounds and oxidants, the potential for chemical transformations and reactions of aromatic compounds to form aerosol and fuel ozone production locally on short time scales (few hours) appears to be particularly high and is important to consider for mitigation strategies.

Bibliography

1. Atkinson, R., and Arey, J.: Atmospheric degradation of volatile organic compounds, Chemical reviews, 103, 4605-4638, 2003.
2. Blake, N. J., Penkett, S. A., Clemitshaw, K. C., Anwyl, P., Lightman, P., Marsh, A. R. W., and Butcher, G.: Estimates of atmospheric hydroxyl radical concentrations from the observed decay of many reactive hydrocarbons in well-defined urban plumes, Journal of Geophysical Research: Atmospheres, 98, 2851-2864, 10.1029/92JD02161, 1993.
3. Bloss, C., Wagner, V., Jenkin, M., Volkamer, R., Bloss, W., Lee, J., Heard, D., Wirtz, K., Martin-Reviejo, M., and Rea, G.: Development of a detailed chemical mechanism (MCMv3. 1) for the atmospheric oxidation of aromatic hydrocarbons, Atmospheric Chemistry and Physics, 5, 641-664, 2005.
4. Bruno, P., Caselli, M., de Gennaro, G., Scolletta, L., Trizio, L., and Tutino, M.: Assessment of the impact produced by the traffic source on VOC level in the urban area of Canosa di Puglia (Italy), Water, air, and soil pollution, 193, 37-50, 2008.
5. Buczynska, A. J., Krata, A., Stranger, M., Godoi, A. F. L., Kontozova-Deutsch, V., Bencs, L., Naveau, I., Roekens, E., and Van Grieken, R.: Atmospheric BTEX-concentrations in an area with intensive street traffic, Atmospheric Environment, 43, 311-318, 2009.
6. Calabrese, E. J., and Kenyon, E.: Air toxics and risk assessment, CRC Press, 1991.
7. Carslaw, D. C., Beevers, S. D., Ropkins, K., and Bell, M. C.: Detecting and quantifying aircraft and other on-airport contributions to ambient nitrogen oxides in the vicinity of a large international airport, Atmospheric Environment, 40, 5424-5434, 2006.
8. De Gouw, J., Goldan, P., Warneke, C., Kuster, W., Roberts, J., Marchewka, M., Bertman, S., Pszenny, A., and Keene, W.: Validation of proton transfer reaction-mass spectrometry (PTR-MS) measurements of gas-phase organic compounds in the atmosphere during the New England Air Quality Study (NEAQS) in 2002, Journal of Geophysical Research: Atmospheres (1984–2012), 108, 2003.

9. De Gouw, J., Middlebrook, A., Warneke, C., Goldan, P., Kuster, W., Roberts, J., Fehsenfeld, F., Worsnop, D., Canagaratna, M., and Pszenny, A.: Budget of organic carbon in a polluted atmosphere: Results from the New England Air Quality Study in 2002, Journal of Geophysical Research: Atmospheres (1984–2012), 110, 2005.
10. Derwent, R. G., Jenkin, M. E., Saunders, S. M., and Pilling, M. J.: Photochemical ozone creation potentials for organic compounds in northwest Europe calculated with a master chemical mechanism, Atmospheric Environment, 32, 2429-2441, http://dx.doi.org/10.1016/S1352-2310(98)00053-3, 1998.
11. Goldstein, A. H., and Galbally, I. E.: Known and unexplored organic constituents in the earth's atmosphere, Environmental Science & Technology, 41, 1514-1521, 2007.
12. Gros, V., Gaimoz, C., Herrmann, F., Custer, T., Williams, J., Bonsang, B., Sauvage, S., Locoge, N., d'Argouges, O., and Sarda-Estève, R.: Volatile organic compounds sources in Paris in spring 2007. Part I: qualitative analysis, Environmental Chemistry, 8, 74-90, 2011.
13. Henze, D., Seinfeld, J., Ng, N., Kroll, J., Fu, T.-M., Jacob, D. J., and Heald, C.: Global modeling of secondary organic aerosol formation from aromatic hydrocarbons: high-vs. low-yield pathways, Atmospheric Chemistry and Physics, 8, 2405-2420, 2008.
14. Hoque, R. R., Khillare, P., Agarwal, T., Shridhar, V., and Balachandran, S.: Spatial and temporal variation of BTEX in the urban atmosphere of Delhi, India, Science of the Total Environment, 392, 30-40, 2008.
15. Jenkin, M. E., Saunders, S. M., Wagner, V., and Pilling, M. J.: Protocol for the development of the Master Chemical Mechanism, MCM v3 (Part B): tropospheric degradation of aromatic volatile organic compounds, Atmos. Chem. Phys., 3, 181-193, 10.5194/acp-3-181-2003, 2003.
16. Karl, T., Jobson, T., Kuster, W. C., Williams, E., Stutz, J., Shetter, R., Hall, S. R., Goldan, P., Fehsenfeld, F., and Lindinger, W.: Use of proton-transfer-reaction mass spectrometry to characterize volatile organic compound sources at the La Porte super site during the Texas Air Quality Study 2000, Journal of Geophysical Research: Atmospheres (1984–2012), 108, 2003.
17. Kato, S., Miyakawa, Y., Kaneko, T., and Kajii, Y.: Urban air measurements using PTR-MS in Tokyo area and comparison with GC-FID measurements, International Journal of Mass Spectrometry, 235, 103-110, 2004.

18. Khoder, M.: Ambient levels of volatile organic compounds in the atmosphere of Greater Cairo, Atmospheric Environment, 41, 554-566, 2007.
19. Koppmann, R.: Volatile organic compounds in the atmosphere, John Wiley & Sons, 2008.
20. Lamb, B., Velasco, E., Allwine, E., Westberg, H., Herndon, S., Knighton, B., and Grimsrud, E.: Ambient VOC measurements in Mexico City during the MCMA 2002 and 2003 field campaigns, Sixth Conference on Atmospheric Chemistry: Air Quality in Megacities, American Meteorol. Soc., Seattle, WA, 2004,
21. Lelieveld, J., Dentener, F., Peters, W., and Krol, M.: On the role of hydroxyl radicals in the self-cleansing capacity of the troposphere, Atmospheric Chemistry and Physics, 4, 2337-2344, 2004.
22. Levy, H.: Normal Atmosphere: Large Radical and Formaldehyde Concentrations Predicted, Science, 173, 141-143, 10.1126/science.173.3992.141, 1971.
23. Lindinger, W., Hansel, A., and Jordan, A.: On-line monitoring of volatile organic compounds at pptv levels by means of proton-transfer-reaction mass spectrometry (PTR-MS) medical applications, food control and environmental research, International Journal of Mass Spectrometry and Ion Processes, 173, 191-241, http://dx.doi.org/10.1016/S0168-1176(97)00281-4, 1998.
24. Liu, J., Mu, Y., Zhang, Y., Zhang, Z., Wang, X., Liu, Y., and Sun, Z.: Atmospheric levels of BTEX compounds during the 2008 Olympic Games in the urban area of Beijing, Science of The Total Environment, 408, 109-116, http://dx.doi.org/10.1016/j.scitotenv.2009.09.026, 2009.
25. Miller, L., Xu, X., Grgicak-Mannion, A., Brook, J., and Wheeler, A.: Multi-season, multi-year concentrations and correlations amongst the BTEX group of VOCs in an urbanized industrial city, Atmospheric Environment, 61, 305-315, http://dx.doi.org/10.1016/j.atmosenv.2012.07.041, 2012.
26. Monks, P. S.: Gas-phase radical chemistry in the troposphere, Chemical Society Reviews, 34, 376-395, 2005.
27. Parrish, D. D., Hahn, C. J., Williams, E. J., Norton, R. B., Fehsenfeld, F. C., Singh, H. B., Shetter, J. D., Gandrud, B. W., and Ridley, B. A.: Indications of photochemical histories of Pacific air masses from measurements of atmospheric trace species at Point Arena, California, Journal of Geophysical Research: Atmospheres, 97, 15883-15901, 10.1029/92JD01242, 1992.

28. Pawar, H., Garg, S., Kumar, V., Sachan, H., Arya, R., Sarkar, C., Chandra, B. P., and Sinha, B.: Quantifying the contribution of long-range transport to Particulate Matter (PM) mass loadings at a suburban site in the North-Western Indo Gangetic Plain (IGP), Atmos. Chem. Phys. Discuss., 15, 11409-11464, 10.5194/acpd-15-11409-2015, 2015.
29. Roberts, J. M., Fehsenfeld, F. C., Liu, S. C., Bollinger, M. J., Hahn, C., Albritton, D. L., and Sievers, R. E.: Measurements of aromatic hydrocarbon ratios and NO x concentrations in the rural troposphere: Observation of air mass photochemical aging and NO x removal, Atmospheric Environment (1967), 18, 2421-2432, 1984.
30. Sarkar, C., Kumar, V., and Sinha, V.: Massive emissions of carcinogenic benzenoids from paddy residue burning in north India, Curr. Sci, 104, 1703-1709, 2013.
31. Sinha, V., Kumar, V., and Sarkar, C.: Chemical composition of pre-monsoon air in the Indo-Gangetic Plain measured using a new air quality facility and PTR-MS: high surface ozone and strong influence of biomass burning, Atmospheric Chemistry and Physics, 14, 5921-5941, 2014.
32. Song, W., Williams, J., Yassaa, N., Martinez, M., Carnero, J., Hidalgo, P., Bozem, H., and Lelieveld, J.: Winter and summer characterization of biogenic enantiomeric monoterpenes and anthropogenic BTEX compounds at a Mediterranean Stone Pine forest site, J Atmos Chem, 68, 233-250, 10.1007/s10874-012-9219-4, 2011.
33. Stone, D., Whalley, L. K., and Heard, D. E.: Tropospheric OH and HO 2 radicals: field measurements and model comparisons, Chemical Society Reviews, 41, 6348-6404, 2012.
34. Warneck, P., and Williams, J.: The Atmospheric Chemist's Companion: Numerical Data for Use in the Atmospheric Sciences, Springer Science & Business Media, 2012.
35. Warneke, C., De Gouw, J. A., Kuster, W. C., Goldan, P. D., and Fall, R.: Validation of atmospheric VOC measurements by proton-transfer-reaction mass spectrometry using a gas-chromatographic preseparation method, Environmental science & technology, 37, 2494-2501, 2003.
36. WorldHealthOrganization: Air quality guidelines for Europe, 2000.
37. Zhang, Y., Wang, X., Barletta, B., Simpson, I. J., Blake, D. R., Fu, X., Zhang, Z., He, Q., Liu, T., Zhao, X., and Ding, X.: Source attributions of hazardous aromatic hydrocarbons in urban, suburban and rural areas in the Pearl River Delta (PRD) region, Journal of Hazardous Materials, 250–251, 403-411, http://dx.doi.org/10.1016/j.jhazmat.2013.02.023, 2013.